Journal of Medicinal Chemistry

ARTICLE

pubs.acs.org/jmc

Discovery and Characterization of 6-{4-[3-(*R*)-2-Methylpyrrolidin-1-yl)propoxy]phenyl}-2*H*-pyridazin-3-one (CEP-26401, Irdabisant): A Potent, Selective Histamine H_3 Receptor Inverse Agonist

Robert L. Hudkins,*[,†] Rita Raddatz,[†] Ming Tao,[†] Joanne R. Mathiasen,[†,#] Lisa D. Aimone,[†] Nadine C. Becknell,[†] Catherine P. Prouty,[†] Lars J. S. Knutsen,[†,⊥] Mehran Yazdanian,[†] Gilbert Moachon,[‡] Mark A. Ator,[†] John P. Mallamo,[†] Michael J. Marino,[†,∥] Edward R. Bacon,[†] and Michael Williams[†,§]

[†]Worldwide Discovery Research and Development, Cephalon, Inc., 145 Brandywine Parkway, West Chester, Pennsylvania 19380, United States

[‡]Cephalon, Inc., 19 Rue Prof. Cadieux, Maisons Alfort, France

Supporting Information

ABSTRACT: Optimization of a novel series of pyridazin-3-one histamine H_3 receptor (H_3R) antagonists/inverse agonists identified 6-{4-[3-(*R*)-2-methylpyrrolidin-1-yl)propoxy]phenyl}-2*H*-pyridazin-3-one (**8a**, CEP-26401; irdabisant) as a lead candidate for potential use in the treatment of attentional and cognitive disorders. **8a** had high affinity for both human (K_i = 2.0 nM) and rat (K_i = 7.2 nM) H_3Rs with greater than 1000-fold selectivity over the hH_1R, hH_2R, and hH_4R histamine receptor subtypes and against an in vitro panel of 418 G-protein-coupled receptors, ion channels, transporters, and enzymes. **8a** demonstrated ideal pharmaceutical properties for a CNS drug in regard to water solubility, permeability and lipophilicity and had low binding to human plasma proteins. It weakly inhibited recombinant cytochrome P450 isoforms and human ether-a-go-go-related gene. **8a** metabolism was minimal in rat, mouse, dog, and human liver microsomes, and it had good interspecies pharmacokinetic properties. **8a** dose-dependently inhibited H_3R agonist-induced dipsogenia in the rat (ED_{50} = 0.06 mg/kg po). On the basis of its pharmacological, pharmaceutical, and safety profiles, **8a** was selected for preclinical development. The clinical portions of the single and multiple ascending dose studies assessing safety and pharmacokinetics have been completed allowing for the initiation of a phase IIa for proof of concept.

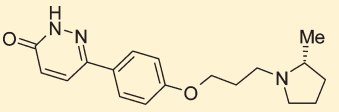

8a

INTRODUCTION

Many drug discovery efforts in the histamine (HIS) G-protein-coupled receptor (GPCR) receptor family, now some 75 years old, are currently focused on the H_3 receptor (H_3R), identified in 1983[1] and finally cloned in 1999.[2] The four receptors (H_1−H_4) that comprise the HIS GPCR family represent one of the more successful drug target classes over the past 50 years, yielding the antihistamines (H_1 blockers) and the H_2-blockers cimetidine and ranitidine. The recently discovered H_4 receptor is expressed mainly in mast cells, eosinophils, and tissues involved in the immune response and may play a role in inflammation and pain.[3] H_3Rs are expressed predominantly on the presynaptic terminals of CNS neurons, and agonist signaling inhibits adenylyl and guanylyl cyclases.[2,4] H_3Rs function as autoreceptors to modulate HIS release[1] and as inhibitory heteroreceptors, regulating the release of key neurotransmitters including acetylcholine, dopamine, norepinephrine, and serotonin that are involved in attention, vigilance, and cognition.[5] Thus, H_3 antagonists may have potential utility in addressing a variety of CNS disorders associated with attention and cognitive deficits, including deficits in wakefulness, attention-deficit hyperactivity disorder (ADHD), Alzheimer's disease (AD), mild cognitive impairment, and schizophrenia.

An important aspect in understanding the role of the H_3R and its ligands is the high degree of constitutive activity in vitro and in vivo.[6] Native and heterologously expressed cloned H_3Rs signal constitutively,[7,8] tonically suppressing neuronal activities, e.g., HIS release, to baseline levels.[6,8] Agonist-induced signaling in the presence of elevated HIS levels further suppresses HIS release. As opposed to H_3 antagonists, which would interfere with HIS-mediated negative feedback, inverse agonists decrease constitutive signaling and suppress tonic inhibition of release, further potentiating histaminergic effects. It has been proposed that H_3R antagonist/inverse agonists may be desirable as therapeutics because of their ability to reverse constitutive activity.[9]

The advancement of new chemical entities (NCEs) in the H_3R field over the past 25 years has been confounded by species differences, interactions with the human ether-a-go-go-related gene (hERG) potassium channel (potential for QTc prolongation and torsade de pointes), and pharmacokinetic (PK) hurdles that include high brain and tissue levels with long residence times, reflecting the potential for tolerance (CNS) and phospholipidosis.[10] Initial work in the field focused on imidazole analogues of the natural ligand, HIS, producing several tool compounds that helped advance the biology, e.g., thioperamide and ciproxifan.[5e,11] To date, however, imidazole-based H_3 antagonists have not

Received: April 4, 2011
Published: June 02, 2011

successfully advanced through the drug development process because of numerous liabilities and poor druglike properties, including metabolic degradation by histamine *N*-methyltransferase (HNMT), poor selectivity, cytochrome P450 (CYP) inhibition, and importantly issues with blood−brain barrier penetration. The search for H_3 antagonists with druglike properties has focused exclusively on amine-based cores. These compounds exhibited reduced side effect liabilities and advanced into clinical evaluation. The phenoxypropylamine pharmacophore is a common H_3 chemotype that had been optimized by several research groups, with substitution of the central phenyl core providing potency and accessory functionality to modulate pharmacokinetics, selectivity, and physical properties.[11,12] Early biphenylphenoxypropylamine candidates, e.g., {4′-[3-((2*R*,5*R*)-2,5-dimethylpyrrolidin-1-yl)propoxy]biphenyl-4-yl}morpholin-4-ylmethanone (**1a**, A-349821) had cognitive enhancing activity in animal models but had low brain permeability and cardiovascular liabilities,[13] and 4′-[3-((*S*)-3-dimethylaminopyrrolidin-1-yl)propoxy]biphenyl-4-carbonitrile (**1b**, A-331440) was positive in an in vitro micronucleus test.[14] A design strategy to rigidify the skeleton to enhance the overall druglike properties and selectivity produced 4-{2-[2-((*R*)-2-methylpyrrolidin-1-yl)ethyl]benzofuran-5-yl}benzonitrile (**1c**, ABT-239).[15] **1c** had an impressive in vivo profile for cognition enhancement but had high plasma protein binding, high brain to plasma partitioning, and the potential to induce phospholipidosis.[16] Its development was ultimately halted because of hERG and cardiovascular liabilities.[16] Merck & Co. advanced 2-methyl-3-[4-(3-pyrrolidin-1-ylpropoxy)phenyl]-5-trifluoromethyl-3*H*-quinazolin-4-one (**2**, MK-0249) as a clinical candidate.[17a,b] **2** had high affinity (hH$_3$ K_i = 1.7 nM) and a good safety profile, but it had poor brain permeability in rodents due to P-glycoprotein (P-gp) mediated efflux.[17] Preclinically, **2** was only effective in promoting histamine release in rat at 30 g/kg po.[17] **2** completed three phase II trails (adult ADHD, treatment of AD, and the cognitive domain of schizophrenia (CDS)); however, it failed to improve cognition in schizophrenia patients dosed for 4 weeks and also failed to improve adult ADHD at 10 mg.[5g] Merck & Co. has advanced a second compound (MK-3134, undisclosed structure) into the clinic for cognition.[5g] 1-{3-[3-(4-Chlorophenyl)propoxy]propyl}piperidine (**3**, BF2.649, pitrolisant) reportedly is in late stage clinical trials for a number of potential indications, including cognitive enhancement, schizophrenia, and antiepileptic activity.[5e,g,18] However, its development and drugability have been questioned, since **3** had limited oral bioavailability, was a potent inhibitor of CYP2D6 and hERG, and had the potential for inducing phospholipidosis.[5d] 6-(3-Cyclobutyl-2,3,4,5-tetrahydro-1*H*-benzo[*d*]azepin-7-yloxy)-*N*-methylnicotinamide (**4**, GSK189254) enhanced cognitive performance preclinically and advanced to phase II for narcolepsy and was in early clinical trials for AD.[19,5d,5e,5g] Reports indicate clinical development on **4** was terminated, and GlaxoSmithKline advanced a second candidate (GSK239512, undisclosed structure) into phase II for treatment of cognitive deficits in AD.[5d−i] Pfizer advanced 3-fluoro-3-(3-fluoro-4-pyrrolidin-1-ylmethylphenyl)cyclobutanecarboxylic acid ethylamide (**1d**, PF-3654746). However, it failed in a phase II ADHD trial and was discontinued.[5g] Early diamine compounds from Johnson & Johnson had exceptionally long bio-half-life and brain residency time and induced phospholipidosis.[5e] The diamine (4-cyclopropylpiperazin-1-yl)-(4-morpholin-4-ylmethylphenyl)methanone (**1e**, JNJ-31001074, bavisant) (Figure 1) completed a phase II ADHD trial, but no results have not been reported.[5k]

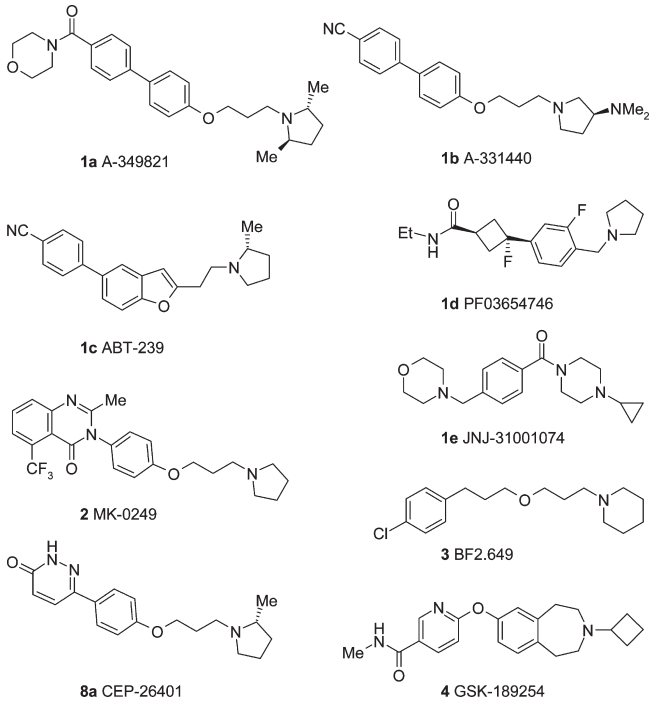

Figure 1. Structures of representative H_3R antagonists.

We have identified a novel class of pyridazin-3-one H_3R antagonists/inverse agonists with excellent drug properties, safety, and in vivo profile. Reported in this paper is the discovery, preliminary structure−activity relationships (SARs), and profile of the potent pyridazin-3-one H_3R clinical candidate 6-{4-[3-(*R*)-2-methylpyrrolidin-1-yl)propoxy]phenyl}-2*H*-pyridazin-3-one (**8a**, CEP-26401, irdabisant).

CHEMISTRY

The synthetic routes for the 6-arylpyridazin-3-one derivatives reported in Table 1 are outlined in Schemes 1−3. The 2*H*-pyridazin-3-one analogues were synthesized using two methods. Method A (Scheme 1) utilizes an aldol/hydrazine cyclocondensation sequence to construct the pyridazinone ring.[20] In the scheme, the aminopropoxy side chain can be efficiently installed either before or after the pyridazinone ring synthesis. Alkylation of 4-hydroxyacetophenone with 3-bromo-1-chloropropane quantitatively produced **6**. Compound **6** was reacted with glyoxalic acid monohydrate in acetic acid at 100 °C, followed by cyclocondensation of the resulting Aldol adduct with hydrazine to give the 2*H*-pyridazin-3-one **7** in 57% yield. Alkylation of chloro **7** with (*R*)-2-methylpyrrolidine produced **8a** in high yield and purity. Analogues **8b**, **8c**, and **8d** were synthesized by first converting chloro **6** to aminoketones **9a**−**c**, which were then subjected to the glyoxalic acid/hydrazine procedure to produce the 2*H*-pyridizan-3-ones. In method B (Scheme 2), a palladium catalyzed Suzuki cross-coupling reaction was used to install the pyridazine moiety. Commercially available 4-(4,4,5,5-tetramethyl[1,3,2]dioxaborolan-2-yl)phenol **10** was alkylated with 3-bromo-1-chloropropane (or 1,3-dibromopropane) to give the chlorodioxaborolane intermediate **11**, which was converted to the versatile aminoborolane reagent (*R*)-2-methyl-1-{3-[4-(4,4,5,5-tetramethyl[1,3,2]dioxaborolan-2-yl)phenoxyl]propyl}pyrrolidine **12** in high yield. Suzuki coupling of **12** with 3,6-dichloropyridazine

Table 1. Pyridazin-3-one in Vitro and PK Data

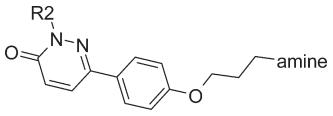

Entry	R2	Amine	hH_3 (K_i nM)	rH_3 K_i nM)	clogP ($logD_{7.4}$)[a]	Rat Pharmacokinetic Parameters[a]			
						i.v. $t_{1/2}$	CL	%F	B/P[f]
1c			9.1 ± 2.8	31 ± 5	5.2	1.5 (5.2)	39 (25)	>18 (53)	32 (36-52)[g]
8a	H		2.0 ± 0.4	7.2 ± 0.4	2.3 (0.6)	2.6	42	83[b]	2.6
8b	H		16 ± 3	50 ± 8	2.3	1.6 ± 0.4	14.5 ± 0.9	25 ± 2[c]	3.1 ± 0.3
8c	H		16 ± 3	45 ± 13	1.9	e			
8d	H		8.7 ± 2.3	37 ± 6	2.5	0.9 ± 0.1	4.9 ± 1.2	11 ± 3[c]	1.9 ± 0.1
8e	H		767 ± 223	822 ± 136	1.3	e			
19a	Me		1.4 ± 0.1	6.3 ± 1.1	2.8 (0.8)	1.6 ± 0.3	45 ± 11	39 ± 2[d]	3.5 ± 0.4
19b	Et		3.9 ± 1.6	11 ± 3	3.5	0.4 ± 0.1	238 ± 73	18 ± 1[c]	1.5 ± 0.1
19c	iPr		4.8 ± 1.3	7.6 ± 2.2	3.6	0.3 ± 0.1	258 ± 195	5 ± 1[c]	2.1 ± 0.1
19d	Ph		2.5 ± 0.9	7.9 ± 1.6	4.3	2.1 ± 0.3	11.7 ± 0.7	10 ± 1[c]	6.2 ± 0.3
19e	Bn		6.9 ± 1.9	12 ± 2	4.6	0.7 ± 0.2	46 ± 31	<1[c]	3.8 ± 0.4
20a	Me		21	106	3.0	1.2 ± 0.4	50 ± 9	22 ± 3[c]	5.3 ± 0.2
20b	Me		9.2 ± 2.8	48 ± 11	1.8	1.0 ± 0.2	90 ± 47	43 ± 3[c]	1.4 ± 0.2
20c	Me		295 ± 57.3	427 ± 123	1.8	e			
21			2.8 ± 0.8	8.5 ± 2.4	2.1	1.0 ± 0.1	9.6 ± 1.7	24 ± 2[d]	1.8 ± 0.2
25			82 ± 23	347 ± 104	2.2	e			

[a] See Experimental Section for methods. Administration at 1 mg/kg iv. $t_{1/2}$ in h. CL in (mL/min)/kg. [b] Protocol as described in Table 3. [c] 5 mg/kg po administration. Calculated from 6 h AUC values. [d] 10 mg/kg po administration. Calculated from 24 h AUC values. [e] Not tested. [f] *B/P* = brain to plasma ratio. [g] Data in parentheses taken from ref 15a.

produced 3-chloropyridazine **13**. Chloro displacement/hydrolysis using sodium acetate in acetic acid at 115 °C cleanly converted 3-chloro **13** to the 2*H*-pyridazin-3-one **8a**. The N^2-substituted derivatives were synthesized as outlined in Scheme 3 by cyclocondensation of 4-(4-methoxyphenyl)-4-oxobutyric acid **14** with various N-substituted hydrazine derivatives.[21] For example, reaction of methylhydrazine and **14** in 2-propanol produced the 2-methyl-4,5-dihydropyridazin-3-one **15a**. Intermediate **15a** was oxidized to **16a** using MnO_2[22a] or $CuCl_2$ in acetonitrile,[22b] then O-demethylated to phenol **17a** with BBr_3 in dichloromethane. The (*R*)-2-methylpyrrolidinylpropoxy side chain was installed by standard conditions via chloro **18a** to give 2-methylpyridazin-3-one **19a**. **19b**−**e** were synthesized in an analogous manner starting with the corresponding N-substituted hydrazine. Amine analogues **20a**−**c** were synthesized from **18a**−**c** as outlined in Scheme 3. The 5-aryl-2*H*-pyridazinone regiomer **21** was synthesized using the Suzuki method coupling dioxaborolane **12** with 2-hydroxymethyl-5-iodo-2*H*-pyridazin-3-one (Scheme 4). Deprotection of the N^2-hydroxymethyl readily occurs in the workup. The N^2-arylpyridazinone regiomer **25** was synthesized by copper mediated

dx.doi.org/10.1021/jm200401v | *J. Med. Chem.* 2011, 54, 4781–4792

Scheme 1[a]

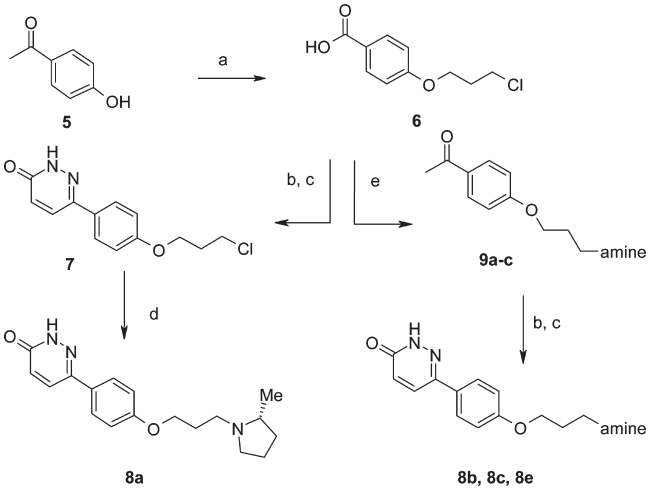

[a] Reagents and conditions: (a) K_2CO_3, 3-bromo-1-chloropropane, acetone, 65 °C, 99%; (b) $CHOCO_2H \cdot H_2O$, HOAc, 100 °C; (c) $N_2H_4-H_2O$, 35−66%, two steps; (d) (*R*)-2-methylpyrrolidine, NaI, K_2CO_3, CH_3CN, 80 °C, 41%; (e) **9a** (*S*)-2-methylpyrrolidine, NaI, CH_3CN, reflux, 93%; **9b** pyrrolidine, NaI, CH_3CN, reflux, 72%; **9c** morpholine, NaI, CH_3CN, reflux, 85%.

Scheme 2[a]

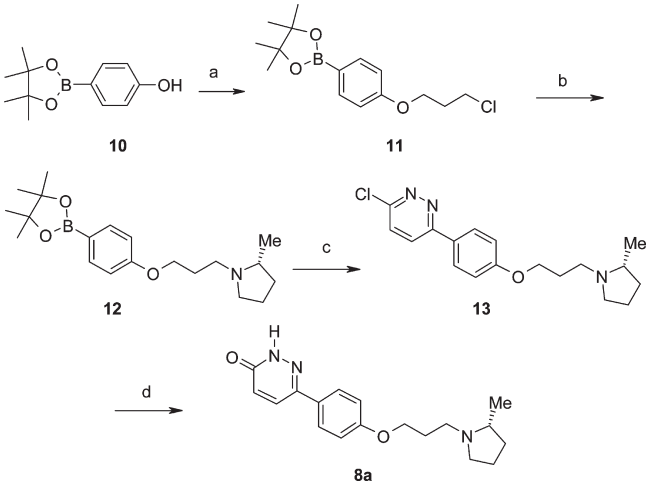

[a] Reagents and conditions: (a) 1-bromo-3-chloropropane, K_2CO_3, CH_3CN; (b) (*R*)-2-methylpyrrolidine, NaI, K_2CO_3, CH_3CN, 80 °C, 65%, two steps; (c) $Pd(OAc)_2$, Ph_3P, 3,6-dichloropyridazine, THF, EtOH, 80 °C, 90%; (d) HOAc, NaOAc 115 °C, 86%.

coupling of (*R*)-1-[3-(4-bromophenoxy)propyl]-2-methylpyrrolidine **24** with 2*H*-pyridazin-3-one as outlined in Scheme 5.

RESULTS AND DISCUSSION

In the lead optimization processes particular attention was placed on issues early in the discovery flow that have plagued the H_3R field, such as high lipophilicity, hERG, and PK, to accelerate the drug discovery process. While important for CNS penetration, lipophilicity contributes significantly to high plasma protein binding, hERG activity and the potential to induce

Scheme 3[a]

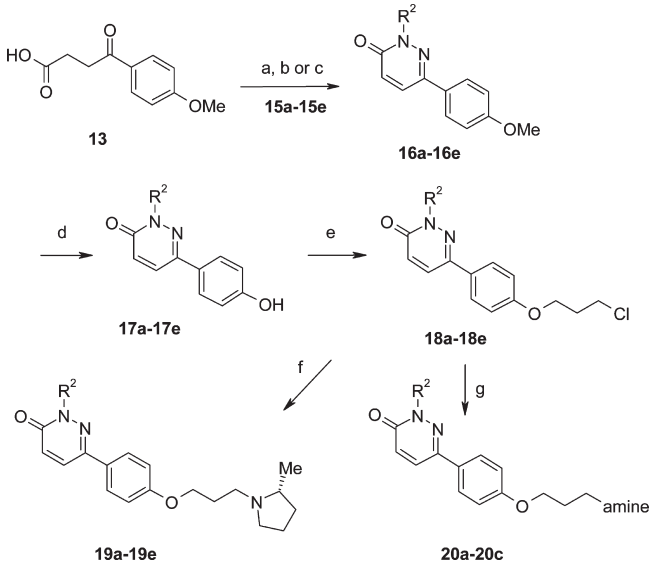

[a] Reagents and conditions: (a) **15a** $MeNHNH_2$; **15b** $EtNHNH_2$; **15c** *i*-$PrNHNH_2$; **15d** $PhNHNH_2$; **15e** $BnNHNH_2$, 2-propanol, reflux; (b) MnO_2, xylenes, 155 °C; (c) Cu(II)Cl_2, CH_3CN, reflux, 71−94%, two steps; (d) BBr_3, DCM, 5 °C → room temp, 92−98%; (e) K_2CO_3, 3-bromo-1-chloropropane, acetone, 65 °C, 78−92%; (f) (*R*)-2-methylpyrrolidine, NaI, K_2CO_3, CH_3CN 80 °C, 48−88%; (g) **20a** piperidine, 71%; **20b** (*S*)-1-pyrrolidin-2-yl-methanol, 53%; **20c** (*R*)-1-pyrrolidin-2-yl-methanol, 50%.

Scheme 4[a]

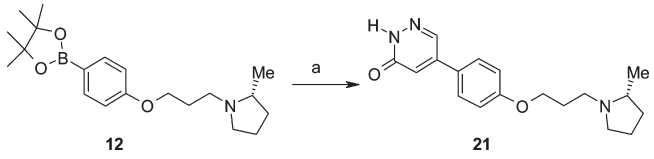

[a] Reagents and conditions: (a) $(PPh_3)_4Pd(0)$, K_2CO_3, 2-hydroxymethyl-5-iodo-2*H*-pyridazin-3-one, DME, reflux 48 h, 63%.

Scheme 5[a]

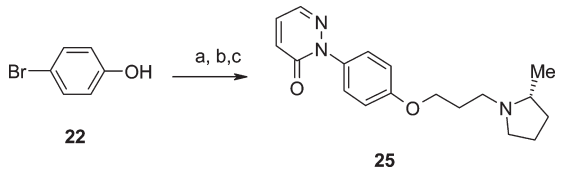

[a] Reagents and conditions: (a) K_2CO_3, 3-bromo-1-chloropropane, acetone, 65 °C, 92%; (b) (*R*)-2-methylpyrrolidine, NaI, K_2CO_3, CH_3CN 80 °C, 97%; (c) 2*H*-pyridazin-3-one, Cu(0), pyr, reflux 18 h, 36%.

phospholipidosis, a toxicity associated with cationic amphiphilic compounds that bind to and accumulate in phospholipid bilayers of cells, causing decreased turnover and accumulation of endosomal and lysosomal phospholipids as lamellar bodies.[10,23] A log *P* criterion of less than 3.0 was set for advancing compounds based on correlations established early in the program with hERG

dx.doi.org/10.1021/jm200401v | *J. Med. Chem.* 2011, 54, 4781–4792

Table 2. Functional and in Vivo Activity for Selected Pyridazin-3-ones

	human GTPγS		rat GTPγS		
compd	K_b, nM[a]	EC_{50}, nM[b]	K_b, nM[a]	EC_{50}, nM[a]	rat dispogenia ED_{50}, mg/kg
8a	0.4 ± 0.1	1.1 ± 0.0	1.1 ± 0.2	2.0 ± 0.8	0.06 (0.01−0.3)[c] 0.01 (0.001−0.08)[d]
19a	0.5 ± 0.1	1.0 ± 0.1	1.1 ± 0.3	2.2 ± 0.6	0.14 (0.1−1.9)[d]
21	0.4 ± 0.2	1.1 ± 0.1	1.3 ± 0.6	2.1 ± 0.2	0.03 (0.02−0.05)[d]

[a] Antagonist. [b] Inverse agonist. [c] po administration. [d] ip administration.

activity and also the propensity for high tissue distribution. In the discovery flow, compounds meeting binding affinity criteria (hH_3 K_i < 15 nM, rH_3 K_i < 50 nM) were screened for selectivity against hH_1, hH_2, and hH_4 receptor subtypes, for aqueous solubility (pH 2 and pH 7.4), in vitro liver microsomal stability (rat, mouse, dog, and human), and inhibition of CYP isoforms (1A2, 2C9, 2C19, 2D6, and 3A4). The selectivity profiles of compounds meeting criteria were further assessed for activity against GPCRs, ion channels, and enzymes. Compounds of interest at this stage were screened in in vivo rat PK experiments designed to evaluate the intrinsic intravenous (iv) PK parameters ($t_{1/2}$, CL, V_d), oral (po) bioavailability and brain partitioning. Those that met criteria for rat PK (and compounds of interest to develop structure−activity relationships) were screened in a functional hERG patch clamp assay for initial assessment of potential QTc liabilities. High quality compounds were then prioritized and advanced into in vivo efficacy models and further PK and safety profiling.

Structure−Activity Relationships. The H_3R SAR was developed using in vitro binding assays by displacement of [^{3}H]*N*-α-methylhistamine ([^{3}H]NAMH) in membranes isolated from CHO cells transfected with cloned human H_3 or rat H_3 receptors.[24] An H_3R binding assay using membranes prepared from rat cortex was used to compare the recombinant rat assay to a native tissue. A summary of the pyridazin-3-one in vitro data in comparison to the reference compound **1c** is shown in Table 1. The SAR for the N^2−H series showed that the (*R*)-2-methylpyrrolidine **8a** had high affinity for both hH_3Rs and rH_3Rs (K_i = 2.0 and 7.2 nM) with a low clogP (2.3). Also, binding affinity of **8a** to rat cortical membranes (K_i = 2.7 ± 0.2 nM) compared favorably to the recombinant rH_3R data. The preference for the *R*-isomer was established early in the project, as the (*S*)-2-methylpyrrolidine isomer **8b** had weaker affinity for hH_3R and rH_3R with eudismic ratios of 8 and 7, respectively (hH_3 K_i = 16 ± 3 nM, rH_3 K_i = 50 ± 8 nM). It is interesting to note that the SAR with **1c** revealed little enantioselectivity between the (*R*)- and (*S*)-2-methylpyrrolidine isomers.[15a,17] The SAR for the amine moiety was further evaluated with a series of amine replacements of the (*R*)-2-methylpyrrolidine. The des-2-methylpyrrolidine **8c** and the piperidine **8d** had 8-fold and 4-fold weaker hH_3R affinity, respectively. The morpholine analogue **8e** had an hH_3 K_i of 767 nM, potentially due to the lower pK_a (7.1) compared to that of **8a** (pK_a = 10.2). The effect of substitution of the N^2-pyridazin-3-one nitrogen showed that significant steric bulk could be accommodated without affecting binding affinity. Methyl **19a**, ethyl **19b**, isopropyl **19c**, and phenyl (**19d**) substitution had essentially equivalent binding affinity for both hH_3R and rH_3R compared to **8a** (Table 1). Although the potency was unaffected, increasing the size of the R^2 group greater than methyl resulted in compounds with clogP values greater than 3, negatively affecting molecular weight and decreasing the ligand efficiency (LE)[25a] and the ligand lipophilic efficiency (LLE).[25b,c] The LLE values for **8a** and **19a** based on the measured log *D* at pH 7.4 were 8.1 and 8.0, respectively. The LE values were as follows: **8a** = 0.52, **19a** = 0.50, **19c** = 0.44, phenyl **19d** = 0.40, and benzyl **19e** = 0.37. The SAR trend for the amine in the N^2-Me series (**19a**) was consistent with the NH series. The piperidine analogue **20a** had 15-fold weaker affinity compared to the (*R*)-2-methylpyrrolidine **19a**. Incorporating an alcohol on the *R*-methylpyrrolidine (**20b**) reduced affinity 7-fold, with the *S*-isomer preferred over *R* (compare **20b** vs **20c**). The position of attachment of the pyridazin-3-one ring to the central phenoxy core was also explored. The 5-pyridazin-3-one regiomer **21** had high affinity (hH_3R K_i = 2.8 nM, rH_3R K_i = 8.5 nM) but lower bioavailability (F = 24%) compared to regiomer **8a**. The N^2-pyridazinone isomer **25** had over 40-fold weaker affinity.

The pyridazin-3-ones were potent antagonists and displayed full inverse agonist activity in the guanosine 5′-(γ-thio)triphosphate ([^{35}S]GTPγS) binding assay[24] (Table 2). Compounds **8a**, **19a**, and **21** potently inhibited *R*-α-methylhistamine (RAMH) induced [^{35}S]GTPγS binding at recombinant rH_3R (**8a** K_b = 1.0 ± 0.2 nM) and hH_3R (**8a** K_b = 0.4 ± 0.1 nM). Compound **8a** decreased basal activity with EC_{50} of 2.0 ± 0.8 and 1.1 ± 0.0 nM for rat and human H_3R, respectively. Inverse agonist data for analogues **19a** and **21** were comparable to data for **8a** (Table 2).

Compounds meeting H_3R affinity and in vitro metabolic stability criteria ($t_{1/2}$ > 40 min) in liver microsomes (data not shown) were screened for pharmacokinetic properties in the rat (Table 1). The N^2-H **8a** showed a $t_{1/2}$ of 2.6 h following iv administration, high systemic clearance, high oral bioavailability (F = 83%), and good brain exposure in the rat (brain to plasma ratio B/P = 2.6). The piperidine **8d** had significantly lower oral bioavailability (F = 11%). The N^2-Me **19a** showed acceptable oral bioavailability (F = 39%) with good brain exposure in the rat (B/P = 3.5). Extensive in vivo PK experiments in rat, dog, and monkey following administration of **19a** showed N-demethylation to the N^2H compound **8a**. On the basis of the presence of the active metabolite **8a**, compound **19a** was not further advanced in discovery and **8a** was selective for advanced testing. The in vivo rat PK SAR indicated that although **19b**−**d** showed acceptable in vitro metabolic stability ($t_{1/2}$ > 40 min in rat liver microsomes), R^2 substituents larger than methyl had poor pharmacokinetics following iv administration with short $t_{1/2}$ and high CL (**19b** and **19c**) or low oral bioavailability (**19d** and **19e**). The F values were based on 6 h of oral AUCs and may be reflective of the high tissue distribution due to the high clogP.

Selectivity of 8a. Compound **8a** had greater than 1000-fold selectivity versus histamine hH_1, hH_2, and hH_4 receptor subtypes (<11% inhibition at 10 μM) and against a panel of 176 GPCRs, ion channels and enzymes (MDS Pharma Services, Seattle, WA). In this panel **8a** had only modest activity at muscarinic M_2 (K_i = 3.7 ± 0.0 μM) and adrenergic α_{1A} (K_i = 9.8 ± 0.3 μM) receptors, dopamine (DAT, K_i = 11 ± 2 μM) and norepinephrine (NET, K_i = 10 ± 1 μM) transporters, and phosphodiesterase PDE3 (IC_{50} = 15 ± 1 μM). **8a** also showed negligible inhibition against 242 kinases (<20% inhibition at 1 μM) and human PARP1 (IC_{50} > 30 μM).[26] Functional inhibition of recombinant human DAT (IC_{50} = 9.4 μM) and NET (IC_{50} = 17.5 μM) was determined, which confirmed weak inhibitory activity for these transporters.

dx.doi.org/10.1021/jm200401v | J. Med. Chem. 2011, 54, 4781–4792

Table 3. Pharmacokinetic Properties of 8a across Species

	rat[a]	dog[b]	monkey[b]
iv $t_{1/2}$ (h)	2.6	2.9	5.4
V_d (L/kg)	9.4	3.5 ± 1.1	3.8 ± 0.9
CL ((mL/min)/kg)	42	13.2 ± 1.5	7.7 ± 1.8
po AUC (ng·h/mL)	984	1190 ± 180	1919 ± 611
C_{max} (ng/mL)	270	230 ± 70	760 ± 74
$t_{1/2}$ (h)	2.9	2.7	5.0
F (%)	83	22 ± 2	83 ± 18
B/P	2.6 ± 0.2	2.4 ± 0.4[c]	*d*

[a] Administered at 1 mg/kg iv and 3 mg/kg po. Parameters were calculated from composite mean plasma concentration−time data (n = 12). [b] Administered at 1 mg/kg iv and 3 mg/kg po for dog and 1 mg/kg iv and po for monkey. Parameters were calculated using plasma concentration−time data for individual animals (dog n = 3; monkey n = 4). [c] Calculated from 5 mg/kg po dose (n = 4). [d] Not determined.

Pharmaceutics Properties of 8a. Both the hydrochloride salt and free base forms were crystalline as assessed by X-ray power diffraction. On the basis of its high water solubility (pH 2 and pH 7.4, >2 mg/mL), the HCl salt form was formulated in saline for in vivo pharmacokinetic and animal studies. The permeability of **8a** (free base) was also evaluated in the Caco-2 intestinal epithelial cell line where it showed high permeability (P_{app} = 13.5 ± 0.9 × 10^{-6} cm/s).[27] The permeability directional ratio (PDR) was less than 2, indicating minimal interaction with efflux transporters such as P-gp. A battery of physicochemical and ADME drug properties were calculated (Tripos, Schrodinger QikProp, ACD Labs) and monitored to aid in the design of NCEs. The log $D_{7.4}$ and clogP calculations provided permeability information on the percent drug that distributed into a nonaqueous lipid layer. **8a** had a clogP of 2.3 (Tripos method) and measured log $D_{7.4}$ of 0.6, in the ideal range for a CNS drug. **8a** was only minimally bound to plasma proteins of rat (39%), dog (32%), and human (44%) in vitro. The unbound fraction in rat brain homogenate,[28a] an important property for CNS in vivo activity,[28b] was also high (40%) and comparable with the unbound fraction found in rat plasma.

Drug Metabolism and Pharmacokinetic Properties of 8a. The in vitro metabolic stability profile of **8a** following incubation with rat, mouse, dog, and human liver microsomes was consistent showing a $t_{1/2}$ greater than 40 min (>98% remaining at 40 min) in each species.[29] Because of the high metabolic stability, an accurate in vitro intrinsic clearance could not be calculated. **8a** inhibited the cytochrome P450 enzymes CYP1A2, 2C9, 2C19, 2D6, and 3A4 with IC_{50} values of greater than 30 μM, indicating minimal potential for drug−drug interactions. **8a** demonstrated low CYP3A4 induction (<2-fold) at concentrations up to 30 μM (Puracyp, Carlsbad, CA).[30]

The interspecies pharmacokinetic properties of **8a** were studied in rat, dog, and monkey (Table 3). The PK parameters for rat shown in Table 3 were calculated from composite mean plasma concentration−time data from 12 rats following administration of 1 mg/kg iv and 3 mg/kg po. The PK parameters for dog (n = 3) and monkey (n = 4) were calculated using plasma concentration−time data for individual animals. Following administration of a single po dose, **8a** was rapidly absorbed with high oral bioavailability in rat and monkey (F = 83%), compared to dog (F = 22%). The iv terminal half-life was 2.6 h in rat, 2.9 h in dog, and 5.4 h in monkey, and **8a** had a moderate clearance in monkey and dog compared to the rat. **8a** was not extensively metabolized in vitro, and a potential explanation for the discrepancy between in vitro and in vivo clearance in rat is a high degree of renal excretion and the fact that the biliary excretion component across species is unknown. The volume of distribution (V_d) in monkey was 3.8 ± 0.9 L/kg with a clearance rate of 7.7 ± 1.8 (mL/min)/kg. The measured brain to plasma ratio was 2.6 in rat and 2.4 in dog. Dose related systemic exposure (C_{max} and AUC) to **8a** was observed after increasing oral doses in each species. Tissue distribution studies with **8a** in male Sprague−Dawley rats were run to determine tissue clearance rate from brain, liver, lung, spleen, kidney, and heart and to evaluate the potential for accumulation as an early indication of phospholipidosis-inducing potential. A single 10 mg/kg po dose of **8a** was cleared in a parallel manner from all tissues and plasma by greater than 98% at 24 h, with low levels of **8a** remaining only in liver, kidney, and spleen.

Drug Safety. As a class, the present H_3R pyridazin-3-one inverse agonists displayed low inhibition of the hERG channel current, a surrogate for the rapidly activating delayed rectifier cardiac potassium current (I_{kr}). The hERG current IC_{50} for **8a** was 13.8 ± 0.8 μM (Cerep, recombinant human hERG/HEK-293 cells). Analogues **19a** and **21** had IC_{50} of 13 and 9.5 μM, respectively. Interaction with the hERG cardiac potassium channel has been implicated in the development of acquired long QT syndrome and a potentially fatal form of ventricular arrhythmia known as torsade de pointes.[31]

8a was nonclastogenic and nonmutagenic and did not induce mutation in the Ames assay in the presence and absence of rat liver S9 metabolic activation. **8a** did not induce micronuclei in vitro in a micronucleus test in cultured human peripheral blood lymphocytes in the presence or absence of metabolic activation (n = 2). **8a** was well tolerated in nonclinical toxicology studies up to 28 days in rats and monkeys, and no issues were observed with cardiovascular safety and respiratory pharmacology in the monkey.

In Vivo Activity in the Rat Dipsogenia Model. The rat dipsogenia model was used as a measure of H_3R blockade in the CNS following peripheral administration of NCEs. Histamine and the H_3-selective agonist RAMH induce water drinking in the rat when administered either peripherally or centrally, an effect blocked by H_3R antagonists.[19,24,32] Activity in this model may be predictive of efficacy in cognitive models.[13,15b,15c,33] **8a** dose-dependently (ED_{50} = 0.01 (0.001−0.08) mg/kg ip; ED_{50} = 0.06 (0.01−0.3) mg/kg po) inhibited RAMH-induced dipsogenia when administered 15 min prior to RAMH. Compounds **19a** and **21** had ED_{50} of 0.01 (0.004−0.03) and 0.03 (0.02−0.05) mg/kg ip, respectively. **8a** was also efficacious in cognition models.[34]

CNS Therapeutic Index. H_3R antagonists/inverse agonists can induce hypothermia, piloerection, loss of righting reflex, irritability, hypoactivity, ptosis, tremors, and even seizures.[15] The CNS side effects of **8a** (10, 30, 100, and 300 mg/kg po) were assessed in the Irwin test, a systematic observational battery that comprehensively assesses behavioral responses to pharmacologic agents[35] at time points from 15 min through 6 h. **8a** was well tolerated and was without side effects at doses up to 100 mg/kg po. The estimated brain concentration at the highest tolerated dose of 100 mg/kg po 1 h postdose was 36 μM, providing a therapeutic index (TI) of >1000 using rat dipsogenia as a quantitative H_3 efficacy model.

CONCLUSION

8a is a novel, orally active, high affinity antagonist/inverse agonist active at human H_3Rs (hH_3R K_i = 2.0 nM) that has

potential for use in the treatment of attentional and cognitive disorders. **8a** had greater than 1000-fold selectivity for the hH_3R over the hH_1R, hH_2R, and hH_4R subtypes and against a panel of 418 GPCRs, ion channels, enzymes, and kinases. **8a** demonstrated "ideal" pharmaceutical properties in regard to water solubility, permeability, and lipophilicity and exhibited low binding to human plasma proteins and weakly inhibited recombinant cytochrome P450 isoforms (1A2, 2C9, 2C19, 2D6, and 3A4) with low induction of CYP3A4, suggesting a minimal potential for drug−drug interactions. In the human hERG functional patch clamp assay, **8a** had an IC_{50} of 14 μM. Metabolism of **8a** was minimal in rat, mouse, dog, and human liver microsomes. **8a** had good pharmacokinetic properties, brain permeability, and safety profile for a CNS-active drug and was selected for full preclinical development. The clinical portions of the single and multiple ascending dose studies assessing safety and pharmacokinetics have been completed allowing for the initiation of a phase IIa proof of concept study.

EXPERIMENTAL SECTION

Chemistry: General Methods. All reagents and anhydrous solvents were obtained from commercial sources and used as received. ^{1}H NMR was obtained on a Bruker 400 MHz instrument in the solvent indicated with tetramethylsilane as an internal standard. Coupling constants (J) are in hertz (Hz). Liquid chromatography−mass spectrometry (LC/MS) were run on a Bruker Esquire 2000 ion trap LCMS. Compound purity was >96% determined by high pressure liquid chromatography (HPLC) using a Zorbax RX-C8, 5 mm × 150 mm column, eluting with a mixture of acetonitrile and water containing 0.1% trifluoroacetic acid with a gradient of 10−100%. Compounds were purified by silica gel chromatography using an ISCO apparatus and monitored at 254 and 290 nm. Melting points were determined using a MEL-TEMP II and are uncorrected. Preparative chromatography was run using silica gel GF 20 mm × 20 cm × 1000 μm plates (Analtech).

Synthesis of 8a. Method A. *1-[4-(3-Chloropropoxy)phenyl]-ethanone (**6**).* A mixture of 1-(4-hydroxyphenyl)ethanone **5** (20.4 g, 150 mmol), K_2CO_3 (62.1 g, 3.0 equiv), and 3-bromo-1-chloropropane (29.6 mL, 2.0 equiv) in acetone (200 mL) was heated to 65 °C overnight. The mixture was cooled to room temperature, filtered, washed with acetone, and concentrated to dryness. The crude product was dissolved in CH_2Cl_2 (150 mL) and washed with saturated $NaHCO_3$ solution, NaCl solution and dried over Na_2SO_4 to give **6** (31.5 g, 99% as an oil). ^{1}H NMR (DMSO-d_6 δ): 2.20 (q, 2H, J = 6.2 Hz), 2.51 (s, 3H), 3.80 (t, 2H, J = 6.2 Hz), 4.19 (t, 2H, J = 6.2 Hz), 7.06 (d, 2H, J = 8.3 Hz), 7.93 (d, 2H, J = 8.3 Hz). LCMS m/z: 213 (M + 1).

*6-[4-(3-Chloropropoxy)phenyl]-2H-pyridazin-3-one (**7**).* A mixture of **6** (10.6 g, 50 mmol) and glyoxalic acid monohydrate (4.6 g, 1.0 equiv) was stirred in acetic acid (15 mL) at 100 °C for 2 h. The solvent was evaporated, 25 mL of water was added, and the mixture was cooled to 0 °C while concentrated NH_4OH was added to pH 8. Hydrazine monohydrate (4.76 mL, 2.0 equiv) was added, and the mixture was heated to 100 °C for 1 h. The reaction was complete by HPLC analysis. The resulting solid was filtered and washed with water. The crude product was dissolved in CH_2Cl_2 (500 mL) and washed with H_2O, 5% $NaHCO_3$ solution, saturated NaCl solution, dried over Na_2SO_4, and purified by ISCO silica gel chromatography (CH_2Cl_2 to 9:1 CH_2Cl_2/MeOH) to give **7** (7.6 g, 57%) as a white solid. Mp 191−193 °C (CH_2Cl_2−MeOH). ^{1}H NMR (DMSO-d_6 δ): 2.16 (q, 2H, J = 6.4 Hz), 3.81 (t, 2H, J = 6.4 Hz), 4.15 (t, 2H, J = 6.4 Hz), 6.95 (1H, d, J = 9.9 Hz), 7.06 (2H, d, J = 7.9 Hz), 7.80 (2H, d, J = 7.8 Hz), 8.0 (1 Hz, d, J = 9.9 Hz). LCMS m/z: 265 (M + 1).

*6-{4-[3-(R)-2-Methylpyrrolidin-1-yl)propoxy]phenyl}-2H-pyridazin-3-one (**8a**).* A mixture of **7** (5.5 g, 21 mmol), K_2CO_3 (10.1 g, 73.5 mmol), NaI (100 mg), and (*R*)-2-methylpyrrolidine hydrochloride (5.1 g, 42 mmol) in acetonitrile (250 mL) was heated at 80 °C for 3 days. The reaction was complete by HPLC analysis. The mixture was filtered, washed with CH_2Cl_2 (2 × 50 mL), and concentrated. The residue was dissolved in CH_2Cl_2 (200 mL) and washed with saturated $NaHCO_3$, saturated NaCl solution, dried with Na_2SO_4, and concentrated. The product was purified by ISCO chromatography using 100% CH_2Cl_2 to 9:1:05 CH_2Cl_2/MeOH/*i*-PrNH_2. The pure product was dissolved in MeOH (15 mL), filtered through 0.45 μm filter, and then 30 mL of 0.5 N HCl in EtOH was added. The solvent was concentrated and the product crystallized from MeOH−ether to give **8a**·HCl (2.65 g, 41%, 99% purity). Mp 240−242 °C (MeOH−ether). ^{1}H NMR (DMSO-d_6 δ): 1.39 (d, 3H, J = 6.8 Hz), 1.64 (m, 1H), 1.95 (m, 2H), 2.17 (m, 5H), 3.07 (m, 2H), 3.40 (m, 2H), 3.61 (m, 1H), 4.15 (m, 2H), 6.96 (d, 1H, J = 10.0 Hz), 7.05 (d, 2H, J = 8.64 Hz), 7.81 (d, 2H, J = 8.64 Hz), 8.0 (d, 1H, J = 10.0 Hz), 10.52 (bs, 1H), 13.08 (s, 1H). LCMS m/z: 314 (M + 1). Anal. ($C_{18}H_{23}ClN_3O_2 \cdot 0.4H_2O$) C, H, N.

Synthesis of 6-{4-[3-(*R*)-2-Methylpyrrolidin-1-yl)propoxy]-phenyl}-2*H*-pyridazin-3-one (8a). Method B. 3-Chloro-6-{4-[3-((*R*)-2-methylpyrrolodin-1-yl)propoxy]phenylpyridazine **13** (0.1 g 0.3 mmol) in 3 mL of glacial acetic acid and sodium acetate (0.027 g, 0.33 mmol) was heated to 115 °C for 2 h. The mixture was cooled to room temperature and then concentrated. The residue was dissolved in EtOAc and washed with saturated $NaHCO_3$, saturated NaCl solution and dried over Na_2SO_4. The product was purified using ISCO silica gel chromatography (EtOAc/EtOH/NH_4OH 9:1:0.5) to give **8a** an off white solid (0.081 g, 86% yield, 98% purity). This compound was identical in its physical and spectral properties to that synthesized by method A.

6-{4-[3-(*S*)-2-Methylpyrrolidin-1-yl)propoxy]phenyl}-2*H*-pyridazin-3-one (8b). To a round-bottom flask was added **9a** (1.8 g, 6.8 mmol), glyoxalic acid hydrate (1.3 g, 13.6 mmol), and acetic acid (10 mL). The mixture was heated at 110 °C for 3 h, cooled to 0 °C, and then diluted with water (25 mL) and NH_4OH solution until pH ∼7 was obtained. To this solution was added hydrazine hydrate (1.0 mL, 20.4 mmol). Then the mixture was heated at 100 °C for 17 h. The mixture was cooled to room temperature, concentrated and the product purified by column chromatography (10% MeOH in CH_2Cl_2) to give 750 mg (35% yield, >99% purity) of **8b**. Mp 156−158 °C. ^{1}H NMR (DMSO-d_6, δ): 0.99 (d, 3H, J = 6 Hz), 1.23−1.32 (m, 1H), 1.59−1.67 (m, 2H), 1.80−1.96 (m, 3H), 2.00−2.14 (m, 2H), 2.20−2.28 (m, 1H), 2.87−2.94 (m, 1H), 3.05−3.10 (m, 1H), 4.07 (t, 2H, J = 5 Hz), 6.95 (d, 1H, J = 10 Hz), 7.02 (d, 2H, J = 8 Hz), 7.78 (d, 2H, J = 9 Hz), 7.98 (d, 1H, J = 10 Hz), 13.0 (s, 1H). LCMS m/z: 314 (M + 1).

6-[4-(3-Pyrrolidin-1-yl-propoxy)phenyl]-2*H*-pyridazin-3-one (8c). To a round-bottom flask was added **9b** (1.3 g, 5.1 mmol), glyoxalic acid hydrate (0.93 g, 10.1 mmol), and acetic acid (8 mL). The reaction was heated at 110 °C for 2 h, cooled to 0 °C, and then diluted with water (25 mL) and NH_4OH solution until pH ∼7 was obtained. To this solution was added hydrazine hydrate (1.0 mL, 20.6 mmol). Then the mixture was heated at 100 °C for 21 h. The mixture was cooled to room temperature, concentrated and the product purified by column chromatography (10% MeOH in CH_2Cl_2) to give 1.0 g (66% yield, 97% purity) of **8c**. Mp 154−157 °C. ^{1}H NMR (DMSO-d_6, δ): 1.68 (broad s, 4H), 1.90 (m, 2H), 2.44 (broad s, 4H), 2.52 (m, 2H), 4.06 (m, 2H), 6.95 (d, 1H, J = 8 Hz), 7.02 (d, 2H, J = 9 Hz), 7.78 (d, 2H, J = 8 Hz), 7.99 (d, 1H, J = 9 Hz), 13.0 (s, 1H). LCMS m/z: 300 (M + 1).

6-[4-(3-Piperidin-1-yl-propoxy)phenyl]-2*H*-pyridazin-3-one (8d). This compound was synthesized by the procedure for **8a**, method B. Yield 54%, purity 98%. Mp 183−184 °C (EtOAc−MeOH). ^{1}H NMR ($CDCl_3$, δ): 1.45 (m, 2H), 1.63 (m, 6H), 2.00 (m, 2H), 2.41 (m, 2H),

2.49 (t, 2H, J = 7.0), 4.06 (t, 2H, J = 7.0), 6.97 (d, 2H, J = 10), 7.03 (d, 1H, J = 10), 7.70 (m, 3H), 11.10 (broad s,1H). LCMS m/z: 314 (M + 1).

6-[4-(3-Morpholin-4-yl-propoxy)phenyl]-2*H*-pyridazin-3-one (8e). To a round-bottom flask was added **9c** (5.0 g, 19.0 mmol), glyoxalic acid hydrate (3.5 g, 47.5 mmol), and acetic acid (15 mL). The mixture was heated at 110 °C for 2.5 h, cooled to 0 °C, and then diluted with water (25 mL) and NH_4OH solution until pH ~6 was obtained. To this solution was added hydrazine hydrate (2.8 mL, 57.0 mmol). Then the mixture was heated at reflux for 20 h (during which time an additional 3 equiv of hydrazine hydrate was added). The mixture was cooled to room temperature, concentrated and the product purified by column chromatography (20% MeOH in CH_2Cl_2) to give 2.53 g (42% yield, 99% purity) of **8e**. Mp 156−159 °C. ^{1}H NMR (DMSO-d_6, δ): 1.89 (m, 2H), 2.37 (broad s, 4H), 2.42 (t, 2H, J = 7 Hz), 3.57 (m, 4H), 4.06 (t, 2H, J = 6 Hz), 6.95 (d, 1H, J = 10 Hz), 7.02 (d, 2H, J = 8 Hz), 7.79 (d, 2H, J = 10 Hz), 7.99 (d, 1H, J = 9 Hz), 13.0 (s, 1H). LCMS m/z: 316 (M + 1).

1-{4-[3-((*S*)-2-Methylpyrrolidin-1-yl)propoxy]phenyl}-ethanone (9a). To a round-bottom flask was added 4′-hydroxyacetophenone **5** (2.0 g, 14.7 mmol), 1-bromo-3-chloropropane (1.5 mL, 15.4 mmol), potassium carbonate (6.1 g, 44.1 mmol), and acetonitrile (50 mL). After the reaction mixture was heated at reflux for 19 h, (*S*)-2-methylpyrrolidine hydrochloride (2.7 g, 22.0 mmol), sodium iodide (2.2 g, 14.7 mmol), and acetonitrile (30 mL) were added. The mixture was stirred at reflux for 24 h and then cooled to room temperature, diluted with CH_2Cl_2 (100 mL), and filtered through a pad of Celite. The filtrate was concentrated and the residue was purified by column chromatography (5% MeOH in CH_2Cl_2) to give **9a** (3.55 g, 93%) as an oil. LCMS m/z: 262 (M + 1).

1-[4-(3-Pyrrolidin-1-yl-propoxy)phenyl]ethanone (9b). To a round-bottom flask was added 4′-hydroxyacetophenone **5** (2.0 g, 14.7 mmol), 1-bromo-3-chloropropane (1.52 mL, 15.4 mmol), potassium carbonate (6.1 g, 44.1 mmol), and acetonitrile (50 mL). After the reaction mixture was heated at 90 °C for 24 h, pyrrolidine (1.84 mL, 22.0 mmol), sodium iodide (2.2 g, 14.7 mmol), and acetonitrile (30 mL) were added. The mixture was stirred at reflux for 24 h, cooled to room temperature, diluted with CH_2Cl_2 (100 mL), and filtered through a pad of Celite. The filtrate was concentrated and the residue was purified by column chromatography (5% MeOH in CH_2Cl_2) to give **9b** (2.60 g, 72%). Mp 146−148 °C. LCMS m/z: 248 (M + 1).

1-[4-(3-Morpholin-4-yl-propoxy)phenyl]ethanone (9c). To a round-bottom flask was added 1-[4-(3-chloropropoxy)phenyl]ethanone (10.0 g, 47.0 mmol), morpholine (6.2 mL, 70.5 mmol), sodium iodide (7.1 g. 47.0 mmol), potassium carbonate (19.5 g, 141 mmol), and acetonitrile (100 mL). The reaction mixture was heated at reflux for 23 h, cooled to room temperature, and diluted with methylene chloride (100 mL). The mixture was then filtered and the filtrate was concentrated and the product purified by column chromatography (2% MeOH in CH_2Cl_2) to give **9c** (10.5 g, 85%) as an off-white solid. Mp 48−51 °C. LCMS m/z: 264 (M + 1).

2-[4-(3-Chloropropoxy)phenyl]-4,4,5,5,-tetramethyl[1,3,2]-dioxaborolane (11). To a round-bottom flask were added 4-(4,4,5,5-tetramethyl[1,3,2]dioxaborolan-2-yl)phenol **10** (11.0 g, 50 mmol), 1-bromo-3-chloropropane (9.9 mL, 100 mmol), potassium carbonate (20.7 g, 150 mmol), and acetonitrile (100 mL). The reaction mixture was heated at reflux for 24 h, cooled to room temperature, and was filtered. The filtrate was concentrated to give **11**. This material was used further without purification.

(*R*)-2-Methyl-1-{3-[4-(4,4,5,5-tetramethyl[1,3,2]dioxaborolan-2-yl)phenoxyl]-propyl}pyrrolidine (12). To a round-bottom flask were added **11**, (*R*)-2-methylpyrrolidine, benzenesulfonic acid salt (24.3 g, 100 mmol), sodium iodide (7.5 g, 50 mmol), potassium carbonate (20.7 g, 150 mmol), and acetonitrile (100 mL). The mixture was heated at reflux for 2.5 days and was cooled to room temperature. The mixture was diluted with methylene chloride (100 mL), filtered, and concentrated. The residue was purified by column chromatography (5% MeOH in CH_2CH_2) to give 11.3 g (65%, two steps) of **12**. Mp 148−150 °C.

3-Chloro-6-{4-[3-((*R*)-2-methylpyrrolidin-1-yl)propoxy]-phenyl}pyridazine (13). $Pd(OAc)_2$ (2.0 g, 9.0 mmol) and Ph_3P (9.4 g, 35.6 mmol) were suspended in anhydrous THF (300 mL) and stirred vigorously under a nitrogen atmosphere for 10 min. 3,6-Dichloropyridazine (26.8 g, 180 mmol) was added and stirred for 10 min. Then **12** (11.8 g, 34 mmol) in THF (200 mL) and EtOH (100 mL) were added dropwise followed by addition of saturated $NaHCO_3$ solution (360 mL). The reaction mixture was heated at 80 °C for 15 h, cooled to room temperature, and evaporated to a solid. This material was dissolved in CH_2Cl_2 (300 mL), washed with water and saturated $NaHCO_3$ solution, then dried (Na_2SO_4) and evaporated. The product was purified by ISCO silica gel chromatography (EtOAc to EtOAc/CH_3OH (9:1) to give **13** (10.2 g, 90%) as an off-white solid. Mp 107−108.5 °C. ^{1}H NMR ($CDCl_3$, δ): 1.10 (d, 3H), 2.99 (m, 2H), 3.18 (m, 2H), 4.10 (m, 2H), 7.04 (d, 2H), 7.50 (d, 1H), 7.78 (d, 1H), 7.99 (d, 2H).

6-(4-Methoxyphenyl)-2-methyl-4,5-dihydro-2*H*-pyridazin-3-one (15a). 4-(4-Methoxyphenyl)-4-oxobutyric acid **14** (27 g, 132 mmol) and methylhydrazine (7.3 g, 8.5 mL, 159 mmol) in 2-propanol (150 mL) were stirred at reflux 12 h. The solvent was concentrated to about 50 mL, and ether was added (~50 mL). The product was collected by filtration, washed with ether, and dried under vacuum to give **15a** (27 g, 94%, purity >96%). Mp 133−135 °C. ^{1}H NMR ($CDCl_3$, δ): 2.57 (m, 2H), 2.9 (m, 2H), 3.4 (s, 3H), 3.8 (s, 3H), 6.9 (d, 2H), 7.6 (d, 2H). LCMS m/z: 218 (M + 1).

6-(4-Methoxyphenyl)-2-methyl-2*H*-pyridazin-3-one (16a). *Method A.* In a 1 L round-bottom flask, **15a** (27 g, 124 mmol) and MnO_2 (30 g, 345 mmol) in xylene (250 mL) were stirred at vigorous reflux for 14 h. The mixture was cooled to room temperature and filtered through a pad of Celite. The xylene was concentrated and the resulting yellow solid was triturated with ether/hexane (1:2) and collected to produce 20 g (75%, 98% purity) of product. The Celite/MnO_2 pad was washed with $CHCl_3$/MeOH 9:1 (2 × 100 mL), filtered, and concentrated. The residue was triturated with ether/hexane (1:2) and collected to give a second crop (4 g, 15%, 96% purity). Total yield of **16a**, 24 g (90%). Mp 109−110 °C. ^{1}H NMR (DMSO-d_6, δ): 3.75 (s, 3H), 3.85 (s, 3H), 7.00−7.05 (m, 3H), 7.82 (d, 2H, J = 9.6 Hz), 8.01 (d, 1H, J = 8.8 Hz). LCMS m/z: 216 (M + 1).

Method B. A mixture of **15a** (3.3 g, 15 mmol) and anhydrous Cu(II)Cl_2 (4.0 g, 2 equiv) in 45 mL of acetonitrile was stirred at reflux for 2 h. The mixture was cooled to room temperature and poured into ice−water (~100 mL). The acetonitrile was removed at reduced pressure, and the resulting off-white solid was collected, washed with water, and crystallized from EtOH−ether to give **16a** (2.5 g, 76%).

6-(4-Hydroxyphenyl)-2-methyl-2*H*-pyridazin-3-one (17a). To **16a** (10 g, 46.3 mmol) in 15 mL DCM cooled on an ice−water bath at ~5 °C was added 93 mL of BBr_3 (1 M solution in DCM) over 5 min. The ice bath was removed and the solution stirred at room temperature for 4 h. The mixture was cooled on an ice bath, and saturated NH_4Cl solution (100 mL) was added slowly. After the addition was complete, the DCM was removed under reduced pressure, excess water added, and the product collected, washed with MeOH (20 mL), and dried to give **17a** (9.2 g, 98%). Mp 242−245 °C. ^{1}H NMR (DMSO-d_6, δ): 3.8 (s, 3H), 6.85 (d, 2H), 7.0 (d, 1H), 7.7 (d, 2H), 7.95 (d, 1H), 9.8 (s, 1H). LCMS m/z: 203 (M + 1).

6-[4-(3-Chloropropoxy)phenyl]-2-methyl-2*H*-pyridazin-3-one (18a). Phenol **17a** (0.5 g, 2.3 mmol), 3-bromo-1-chloropropane (0.7 g, 4.6 mmol), and K_2CO_3 (1.0 g) in CH_3CN (25 mL) was stirred at reflux 20 h. The mixture was filtered and concentrated. The resulting oil was dissolved in Et_2O and washed with water, NaCl solution, dried ($MgSO_4$), and concentrated. The product was triturated with

Et_2O−hexanes to yield **18a** (0.6 g, 91%). Mp 186−187 °C. ^{1}H NMR (DMSO-d_6, δ): 2.2 (m, 2H, J = 7 Hz), 3.7 (s, 3H), 3.8 (t, 2H, J = 7 Hz), 4.15 (t, 2H, J = 7 Hz), 7.0−7.1 (m, 3H), 7.8 (d, 2H, J = 7.8 Hz), 8.0 (d, 1H). LCMS m/z: 279 (M + 1).

2-Methyl-6-{4-[3-((*R*)-2-methylpyrrolidin-1-yl)propoxy]-phenyl}-2*H*-pyridazin-3-one (19a). A mixture of **18a** (1.5 g, 5.4 mmol), K_2CO_3 (2.2 g 16.2 mmol), NaI (0.8 g, 5.4 mmol), (*R*)-2-methylpyrrolidine−HCl (1.3 g, 10.8 mmol) in CH_3CN (30 mL) was heated under N_2 at 90 °C for 2 days. The mixture was filtered and concentrated. The residue was dissolved in EtOAc and washed with 2 N Na_2CO_3, NaCl solution, dried ($MgSO_4$), and concentrated. The product was purified by ISCO silica gel chromatography (95:5 DCM/MeOH). The fractions were combined and concentrated to yield **19a** (0.85 g, 48%, free base). The HCl salt was prepared by adding a 1 N HCl−ether solution to the base in ether. The white solid was collected and crystallized from CH_3CN−ether. Mp 183−185 °C. ^{1}H NMR (DMSO-d_6, δ): 1.38 (d, 3H, J = 5.2 Hz), 1.62 (m, 1H), 1.92−1.97 (m, 2H), 2.1−2.3 (m, 3H), 3.1 (m, 2H), 3.4 (m, 2H), 3.6 (m, 1H), 3.7 (m, 1H), 3.7 (s, 3H), 4.15 (m, 2H), 7.0−7.17 (m, 3H), 7.8 (d, 2H, J = 8.6 Hz), 8.0 (d, 1H, J = 9.6 Hz), 10.1 (s, 1H). LCMS m/z: 328 (M + 1).

Compounds **19b-e** and **20a−c** were synthesized using the methods for **19a**.

2-Ethyl-6-{4-[3-((*R*)-2-methylpyrrolidin-1-yl)propoxy]phenyl}-2*H*-pyridazin-3-one (19b). Yield 96% free base, purity 97%. Mp 58−62 °C (L-tartrate salt, acetone−ether). ^{1}H NMR (DMSO-d_6 δ): 1.19 (d, 3H, J = 5.6 Hz), 1.29−1.33 (t, 3H, J = 7.1 Hz), 1.4 (m, 1H), 1.7 (m, 2H), 2.0 (m, 4H), 2.8 (m, 2H), 3.0 (broad, 1H), 3.2 (broad, 1H), 6.99−7.06 (m, 3H), 7.84 (d, 1H, J = 8.9 Hz), 7.99 (d, 2H, J = 9 Hz). LCMS m/z: 342 (M + 1).

2-Isopropyl-6-{4-[3-((*R*)-2-methylpyrrolidin-1-yl)propoxy]-phenyl}-2*H*-pyridazin-3-one (19c). Yield 88% free base, purity 98%. Mp 60−64 °C (L-tartrate salt, $CHCl_3$−ether−hexane). ^{1}H NMR ($CDCl_3$, δ): 1.09 (d, 3H, J = 5.8 Hz), 1.43 (d, 6H, J = 6.6 Hz), 1.7−1.9 (m, 2H), 1.9−2.4 (m, 7H), 2.8 (m, 1H), 3.0 (broad, 1H), 4.06−4.1 (m, 2H), 5.37 (m, 1H), 6.94−6.99 (m, 3H), 7.59 (d, 1H, J = 9.7 Hz), 7.73 (d, 2H, J = 8.7 Hz). LCMS m/z: 358 (M + 1).

2-Phenyl 6-{4-[3-((*R*)-2-Methylpyrrolidin-1-yl)propoxy]-phenyl}-2*H*-pyridazin-3-one (19d). Yield 88% purity 96%. Mp 82−86 °C (CH_2Cl_2). ^{1}H NMR (DMSO-d_6, δ): 1.36 (m, 3H), 1.59 (m, 1H), 1.91 (m, 2H), 2.14 (m, 3H), 3.09 (m, 2H), 3.39 (m, 2H), 3.59 (m, 1H), 4.13 (t, 2H, J = 4.5 Hz), 7.06 (d, 2H, J = 8.5 Hz,), 7.16 (d, 1H, J = 9.8 Hz,), 7.44 (t, 1H, J = 6.9 Hz,), 7.53 (t, 2H, J = 7.9 Hz,), 7.65 (d, 2H, J = 8.3 Hz,), 7.88 (d, 2H, J = 8.5 Hz,), 8.13 (d, 1H, J = 9.8 Hz,). LCMS m/z: 390 (M + 1).

2-Benzyl-6-{4-[3-((*R*)-2-Methylpyrrolidin-1-yl)propoxy]-phenyl}-2*H*-pyridazin-3-one (19e). Yield 88% free base, purity 96%. Mp 228−230 °C (HCl salt, MeOH−ether). ^{1}H NMR (DMSO-d_6, δ): 1.37 (d, 3H, J = 6.2 Hz), 1.62 (m, 1H), 1.94 (m, 2H), 2.15 (m, 3H), 3.12 (m, 2H), 3.44 (m, 2H), 3.62 (m, 1H), 4.13 (t, 2H, J = 5.8 Hz), 5.31 (s, 2H), 7.07 (m, 3H), 7.31 (m, 3H), 7.35 (d, 2H, J = 4.1 Hz), 7.85 (d, 2H, J = 8.7 Hz), 8.04 (d, 1H, J = 9.5 Hz), 9.53 (broad s, 1H). LCMS m/z: 404 (M + 1).

2-Methyl-6-[4-(3-piperidin-1-yl-propoxy)phenyl]-2*H*-pyridazin-3-one (20a). Yield 71%, purity 98%. Mp 200−201 °C (HCl salt, MeOH−ether). ^{1}H NMR ($CDCl_3$, δ): 1.58−161 (br m, 6H), 2.00−2.04 (m, 2H), 2.4 (b, 4H), 2.47−2.51 (m, 2H), 3.86 (s, 3H), 4.06 (m, 2H), 6.95−7.0 (m, 3H), 7.63 (d, 1H, J = 9.7 Hz), 7.70 (d, 2H, J = 7 Hz). LCMS m/z: 328 (M + 1).

6-{4-[3-((*S*)-2-Hydroxymethyl-pyrrolidin-1-yl)propoxy]-phenyl}-2-methyl-2*H*-pyridazin-3-one Hydrochloride (20b). Yield 53%, purity 99%. Mp 169 °C (HCl salt, acetonitrile−hexanes). ^{1}H NMR (DMSO-d_6 δ): 1.78 (broad m, 1H), 1.90 (broad m, 1H), 2.07 (broad m, 1H), 2.10 (broad m, 1H), 2.25 (broad m, 2H), 3.09−3.20 (broad m, 2H), 3.58 (broad m, 3 H), 3.68 (m, 1H), 3.72 (s, 3H), 3.78 (m, 1H), 4.14 (t, 2H, J = 5.9 Hz), 5.45 (br s, 1H), 7.06 (m, 3H), 7.85 (d, 2H, J = 8.4 Hz), 8.03 (d, 1H, J = 9.7 Hz), 10.09 (br s, 1H). LCMS m/z: 344 (M + 1).

6-{4-[3-((*R*)-2-Hydroxymethylpyrrolidin-1-yl)propoxy]-phenyl}-2-methyl-2*H*-pyridazin-3-one Hydrochloride (20c). Yield 50%, purity 99%. Mp 166−167 °C (HCl salt, acetonitrile−hexanes). ^{1}H NMR (DMSO-d_6 δ): 1.78 (broad m, 1H), 1.90 (broad m, 1H), 2.07 (broad m, 1H), 2.10 (broad m, 1H), 2.24 (broad m, 2H), 3.12−3.20 (broad m, 2H), 3.59 (broad m, 3H), 3.68 (m, 1H), 3.72 (s, 3H), 3.75 (m, 1H), 4.14 (t, 2H, J = 5.9 Hz), 5.45 (broad s, 1H), 7.06 (m, 3H), 7.85 (d, 2H, J = 8.7 Hz), 8.03 (d, 1H, J = 9.7 Hz), 10.09 (broad s, 1H). LCMS m/z: 344 (M + 1).

5-{4-[3-((*R*)-2-Methylpyrrolidin-1-yl)propoxy]phenyl}-2*H*-pyridazin-3-one (21). To a round-bottom flask was added **12** (3.3 g, 9.5 mmol), 2-hydroxymethyl-5-iodo-2*H*-pyridazin-3-one (2.3 g, 9.1 mmol), tetrakis(triphenylphosphine)palladium(0) (2.1 g, 1.8 mmol), potassium carbonate (6.3 g, 45.2 mmol), 1,2-dimethoxyethane (80 mL), and water (40 mL). The reaction mixture was flushed with nitrogen for 30 min and was heated at reflux for 48 h. The mixture was cooled to room temperature, filtered, and concentrated. The residue was purified by column chromatography (CH_2Cl_2/MeOH/*i*-$PrNH_2$, 9:1:0.1) to give **21** (3.3 g, 63% yield, 98% purity). Mp 166−169 °C. ^{1}H NMR (DMSO-d_6, δ): 1.00 (d, 3H, J = 4 Hz), 1.27−1.3.6 (m, 1H), 1.56−1.72 (m, 1H), 1.87 (m, 3H), 1.98−2.29 (m, 3H), 2.84−2.98 (m, 1H), 3.03−3.13 (m, 1H), 4.09 (t, 2H, J = 6 Hz), 7.06 (m, 2H), 7.78 (m, 3H), 8.29 (m, 2H), 13.0 (s, 1H). LCMS m/z: 314 (M + 1).

1-Bromo-4-(3-chloropropoxy)benzene (23). 4-Bromophenol **22** (10 g, 57.8 mmol), 3-bromo-1-chloropropane (9.6 g, 60.7 mmol), and K_2CO_3 (8.0 g, 63.6 mmol) in acetone was stirred at reflux for 18 h. The mixture was cooled to room temperature, filtered, and concentrated at reduced pressure. The resulting oil was dissolved in ether (100 mL) and washed with 1 N NaOH solution (2 × 25 mL), water, NaCl solution and dried over $MgSO_4$ to give **23** (13.3 g, 92%) as a clear oil that solidified on standing. ^{1}H NMR (DMSO-d_6, δ): 2.21 (m, 2H), 3.73 (t, 2H, J = 6.1 Hz), 4.08 (t, 2H, J = 5.7 Hz), 6.78 (d, 2H, J = 8 Hz), 7.37 (d, 2H, J = 8 Hz). LCMS m/z: 250 (M + 1).

(*R*)-1-[3-(4-Bromophenoxy)propyl]-2-methylpyrrolidine (24). A mixture of **22** (2.0 g, 8.0 mmol), (*R*)-2-methylpyrrolidine−HCl (1.2 g, 9.6 mmol), K_2CO_3 (2.2 g, 16 mmol), and NaI (0.6 g, 4 mmol) in acetonitrile (35 mL) was stirred at reflux 48 h. The mixture was cooled to room temperature. Water was added and the solution extracted with ether (3 × 25 mL). The ether layer was washed with water, NaCl solution and dried over $MgSO_4$ to give **23** (2.3 g, 97%) as a clear oil. The HCl salt was prepared by adding a 1 N HCl−ether solution to the base in ether. Mp 157−159 C (HCl salt, MeOH−ether). ^{1}H NMR ($CDCl_3$, δ): 1.07 (d, 3H, J = 6 Hz), 1.39−1.43 (m, 1H), 1.66−1.79 (m, 2H), 1.87−2.00 (m, 3H), 2.06−2.21 (m, 2H), 2.26−2.31 (m, 1H), 2.92−2.99 (m, 1H), 3.14−3.18 (m, 1H), 3.97−4.0 (m, 2H), 6.77 (d, 2H, J = 8 Hz), 7.35 (d, 2H, J = 8 Hz). LCMS m/z: 299 (M + 1).

2-{4-[3-((*R*)-2-Methylpyrrolidin-1-yl)propoxy]phenyl}-2*H*-pyridazin-3-one (25). A mixture of **24** (560 mg, 1.87 mmol), 2*H*-pyridazin-3-one (180 mg, 1.87 mmol), K_2CO_3 (775 mg, 5.61 mmol), copper powder (120 mg, 1.87 mmol) in pyridine (75 mL) was stirred at reflux under nitrogen for 18 h. The mixture was cooled to room temperature and concentrated at reduced pressure. The residue was absorbed onto Fluorosil for elution and purification by ISCO silica gel chromatography (95:5:1/DCM, MeOH, *i*-$PrNH_2$). The fractions containing pure product were collected and concentrated. The solid was crystallized from Et_2O−hexanes to give **25** (210 mg, 36%, 97% purity) as a white solid. Mp 106−107 °C. The HCl salt was prepared by dissolving the base in MeOH and adding 1 N Et_2O−HCl. After concentration the product was crystallized using MeOH−ether. Mp 175−177 °C (MeOH−Et_2O). ^{1}H NMR ($CDCl_3$, δ): 1.10 (d, 3H, J = 5.2 Hz), 1.42 (m, 1H), 1.70−1.79 (m, 2H), 1.79−1.92 (m, 3H), 2.11−2.30 (m, 3H), 2.98 (m, 1H), 3.18 (m, 1H), 4.06 (m, 2H), 6.98 (d, 2H, J = 8 Hz), 7.04 (d, 1H, J = 9 Hz), 7.21−7.24 (m, 1H), 7.50 (d, 2H, J = 8 Hz), 7.87 (s, 1H). LCMS m/z: 314 (M + 1).

Pharmacokinetics. Adult male Sprague−Dawley rats (275−350 g; Charles River, Kingston, NY), male beagle dogs (9−14 kg, Cephalon, Inc., Maisons Alfort, France), and male cynomolgus monkeys (2−4 kg, Covance Laboratories, Alice, TX) were used in the experiments. All animal usage was approved by the Cephalon IUCAC. For routine compound screening rats were dosed via the lateral tail vein at the indicated dose for iv administration (3% DMSO, 30% Solutol, 67% phosphate buffered saline or 100% saline) or via oral gavage (50% Tween 80, 40% propylene carbonate, and 10% propylene glycol, saline, or 2% HCl−water) at the indicated dose. Rats were fasted overnight prior to po administration. Serial blood samples were collected from the lateral tail vein into heparinized collection tubes (approximately 0.25 mL) at seven sampling times over a 6 or 24 h period as indicated. The plasma was separated by centrifugation, and the sample was prepared for analysis HPLC/MS by protein precipitation with acetonitrile. The plasma samples were analyzed for drug and internal standard via LC−MS/MS protocol. The pharmacokinetic parameters were calculated by a noncompartmental method using WinNonlin software (Professional version 4.1, Pharsight Corporation, Palo Alto, CA, 1997). For experiments to determine detailed rat PK parameters, rats were administered 1 mg/kg iv and 3 mg/kg po in saline and parameters calculated from composite mean plasma concentration−time data (n = 12).

Dogs were administered at 1 mg/kg iv and 3 mg/kg po and monkeys at 1 mg/kg iv and po. Parameters were calculated using plasma concentration−time data for individual animals (dog n = 3; monkey n = 4).

Plasma Protein Binding. Test compounds were dissolved in DMSO and spiked into plasma from rat, dog, and human, as well as phosphate-buffered saline (pH 7.4). The final concentration in plasma or PBS was 5 μM. The mixtures were incubated in a 37 °C water bath with gentle shaking for 1 h and then were loaded into the MultiScreen Ultracell-PPB plate (Millipore Inc., Billerica, MA) that was centrifuged at 2000g for 45 min at 37 °C. The amount of compound present in the ultrafiltrate was determined using LC/MS/MS. The percentage of drug bound to plasma was calculated using mean peak area of test compound in plasma ultrafiltrate (as free) and mean peak area of compound in PBS buffer (as total). The results are the mean of duplicate determinations.

Rat Dipsogenia Model. Rat dipsogenia was conducted as previously described.[24,32] RAMH-induced water intake was measured in Harlan Long Evans rats (>300 g; Harlan, Dublin, VA, or Indianapolis, IN) for 30 min beginning 20 min after administration of RAMH (10 mg/kg ip). Test compound (in saline) was administered at the indicated times prior to the initiation of the drinking trial period. Percent inhibition of RAMH-induced drinking was calculated for each rat based on normalization to the group mean RAMH-induced drinking using the following equation: $[100 - (\mathrm{Dr}/(\mathrm{Dg}_{\mathrm{RAMH}})) \times 100]$, where Dr is the amount of water an individual rat drinks and $\mathrm{Dg}_{\mathrm{RAMH}}$ is the group mean for the amount of water consumed by the RAMH-treated group. Group mean values for percent inhibition were then calculated for each dosage group together with the associated standard deviation and standard error of the mean. Treatment effects for percent inhibition vs RAMH-induced dipsogenia were evaluated using a one-way ANOVA (GraphPad Prism 4). Dunnett's post hoc analysis was performed for multiple comparisons with the RAMH group set as the control comparator.

■ ASSOCIATED CONTENT

Supporting Information. Elemental analysis results of **8a**. This material is available free of charge via the Internet at http://pubs.acs.org.

■ AUTHOR INFORMATION

Corresponding Author

*Phone: 610-738-6283. Fax: 610-738-6558. E-mail: rhudkins@cephalon.com.

Present Addresses

[§]Department of Molecular Pharmacology and Biological Chemistry, Feinberg School of Medicine, Northwestern University, Chicago, IL.

[∥]Merck & Co. Inc., West Point, PA.

[⊥]Discovery Pharma, LLC, West Chester, PA.

[#]Department of Pharmaceutical Sciences, School of Pharmacy, Thomas Jefferson University, Philadelphia, PA.

■ ACKNOWLEDGMENT

The authors acknowledge the support and contributions from Véronique Agathon, Brad Barnes, Bob Bendesky, Nathalie Bourrit, Donna Bozyczko-Coyne, Amy Decamillo, Debra Galinis, Sébastien Girault, John Gruner, Ed Hellriegel, Zeqi Huang, Kurt Josef, Isabelle Kanmacher, Siyuan Le, Nicole Lepallec, Brigitte Lesur, Jackie Lyons, Val Marcy, Phil Robertson, Xiu Ping Wang, and Allison Zulli.

■ ABBREVIATIONS USED

hH_1R, human H_1 receptor; hH_2R, human H_2 receptor; hH_4R, human H_4 receptor; H_3R, H_3 receptor; GPCR, G-protein-coupled receptor; HIS, histamine; ADHD, attention-deficit hyperactivity disorder; AD, Alzheimer's disease; NCE, new chemical entities; hERG, human ether-a-go-go-related gene; HNMT, histamine *N*-methyltransferase; SAR, structure−activity relationship; PK, pharmacokinetics; [^{3}H]NAMH, [^{3}H]*N*-α-methylhistamine; LE, ligand efficiency; LLE, ligand lipophilic efficiency; [^{35}S]GTPγS, guanosine 5′-(γ-thio)triphosphate; RAMH, *R*-α-methylhistamine; TI, therapeutic index; CDS, cognitive domain of schizophrenia; P-gp, P-glycoprotein

■ REFERENCES

(1) Arrang, J. M.; Garbarg, M.; Schwartz, J. C. Auto-inhibition of brain histamine release mediated by a novel class (H_3) of histamine receptor. *Nature* **1983**, *302*, 832–837.

(2) Lovenberg, T. W.; Roland, B. L.; Wilson, S. J.; Jiang, X.; Pyati, J.; Huvar, A.; Jackson, M. R.; Erlander, M. G. Cloning and functional expression of the human histamine H_3 receptor. *Mol. Pharmacol.* **1999**, *55*, 1101–1107.

(3) (a) Leurs, R.; Chazot, P. L.; Shenton, F. C.; Lim, H. D.; de Esch, I. J. Molecular and biochemical pharmacology of the histamine H4 receptor. *Br. J. Pharmacol.* **2009**, *157*, 14–23. (b) Zampeli, E.; Tiligada, E. The role of histamine H4 receptor in immune and inflammatory disorders. *Br. J. Pharmacol.* **2009**, *157*, 24–33. (c) Oda, T.; Morikawa, N.; Saito, Y.; Masuho, Y.; Matsumoto, S. Molecular cloning and characterization of a novel type of histamine receptor preferentially expressed in leukocytes. *J. Biol. Chem.* **2000**, *275*, 36781–36786. (d) Kiss, R.; Keseru, G. M. Histamine H4 receptor ligands and their potential therapeutic applications. *Expert Opin. Ther. Pat.* **2009**, *19*, 119–135.

(4) (a) Bongers, G.; Bakker, R. A.; Leurs, R. Molecular aspects of the histamine H_3 receptor. *Biochem. Pharmacol.* **2007**, *73*, 1195–1204. (b) Wulff, B. S.; Hastrup, S.; Rimvall, K. Characteristics of recombinantly expressed rat and human histamine H_3 receptors. *Eur. J. Pharmacol.* **2002**, *453*, 33–41.

(5) Reviews: (a) Leurs, R.; Bakker, R. A.; Timmerman, H.; de Esch, I. J. The histamine H_3 receptor: from gene cloning to H_3 receptor drugs. *Nat. Rev. Drug Discovery* **2005**, *4*, 107–120. (b) Wijtmans, M.; Leurs, R.; de Esch, I. Histamine H_3 receptor ligands break ground in a remarkable plethora of therapeutic areas. *Expert Opin. Invest. Drugs* **2007**, *16*, 967–985. (c) Esbenshade, T. A.; Fox, G. B.; Cowart, M. D. Histamine H_3 receptor antagonists: preclinical promise for treating obesity and cognitive disorders. *Mol. Interventions* **2006**, *6*, 77–88. (d) Esbenshade, T. A.; Browman, K. E.; Bitner, R. S.; Strakhova, M.; Cowart, M. D.;

Brioni, J. D. The histamine H_3 receptor: an attractive target for the treatment of cognitive disorders. *Br. J. Pharmacol.* **2008**, *154*, 1166–1181. (e) Hudkins, R. L.; Raddatz, R. Recent advances in drug discovery of histamine H_3 antagonist. *Annu. Rep. Med. Chem.* **2007**, *42*, 49–63. (f) Sander, K.; Kottke, T.; Stark, H. Histamine H_3 receptor antagonists go to clinics. *Biol. Pharm. Bull.* **2008**, *31*, 2163–2181. (g) Brioni, J. D.; Esbenshade, T. A.; Garrison, T. R.; Bitner, S. R.; Cowart, M. D. Discovery of histamine H3 antagonists for the treatment of cognitive disorders and Alzheimer's disease. *J. Pharmacol. Exp. Ther.* **2011**, *336*, 38–46. (h) Raddatz, R.; Tao, M.; Hudkins, R. L. Histamine H3 antagonists for treatment of cognitive deficits in CNS diseases. *Curr. Top. Med. Chem.* **2010**, *10*, 153–169. (i) Berlin, M.; Boyce, C. W.; de Lera Ruiz, M. Histamine H(3) receptor as a drug discovery target. *J. Med. Chem.* **2011**, *54*, 26–53. (j) Celanire, F.; Lebon, F.; Stark, H. Drug Discovery: From Hits to Clinical Candidates. In *The Third Histamine Receptor: Selective Ligands as Potential Therapeutic Agents in CNS Disorders*; Vohora, D., Ed.; CRC Press: Boca Raton, FL, 2009. (k) Thompson Reuters Integrity, Bavisant, Entry 470497, 2011. (l) See trials NCT00675090, NCT00420420, NCT00506077, NCT00531752; www.clinicaltrials.gov.

(6) Arrang, J. M.; Morisset, S.; Gbahou, F. Constitutive activity of the histamine H_3 receptor. *Trends Pharmacol. Sci.* **2007**, *28*, 350–357.

(7) Morisset, S.; Rouleau, A.; Ligneau, X.; Gbahou, F.; Tardivel-Lacombe, J.; Stark, H.; Schunack, W.; Ganellin, C. R.; Schwartz, J. C.; Arrang, J. M. High constitutive activity of native H_3 receptors regulates histamine neurons in brain. *Nature* **2000**, *408*, 860–864.

(8) Wieland, K.; Bongers, G.; Yamamoto, Y.; Hashimoto, T.; Yamatodani, A.; Menge, W. M.; Timmerman, H.; Lovenberg, T. W.; Leurs, R. Constitutive activity of histamine h(3) receptors stably expressed in SK-N-MC cells: display of agonism and inverse agonism by H(3) antagonists. *J. Pharmacol. Exp. Ther.* **2001**, *299*, 908–914.

(9) Schwartz, J. C.; Morisset, S.; Rouleau, A.; Ligneau, X.; Gbahou, F.; Tardivel-Lacombe, J.; Stark, H.; Schunack, W.; Ganellin, C. R.; Arrang, J. M. Therapeutic implications of constitutive activity of receptors: the example of the histamine H_3 receptor. *J. Neural Transm., Suppl.* **2003**, *64*, 1–16.

(10) Reasor, M. J.; Hastings, K. L.; Ulrich, R. G. Drug-induced phospholipidosis: issues and future directions. *Expert Opin. Drug Saf.* **2006**, *5*, 567–583.

(11) (a) Stark, H.; Kathmann, M.; Schlicker, E.; Schunack, W.; Schlegel, B.; Sippl, W. Medicinal chemical and pharmacological aspects of imidazole-containing histamine H_3 receptor antagonists. *Mini-Rev. Med. Chem.* **2004**, *4*, 965–977. (b) Letavic, M. A.; Barbier, A. J.; Dvorak, C. A.; Carruthers, N. I. Recent medicinal chemistry of the histamine H_3 receptor. *Prog. Med. Chem.* **2006**, *44*, 181–206.

(12) (a) Stocking, E. M.; Letavic, M. A. Histamine H_3 antagonists as wake-promoting and pro-cognitive agents. *Curr. Top. Med. Chem.* **2008**, *8*, 988–1002. (b) Cowart, M.; Altenbach, R.; Black, L.; Faghih, R.; Zhao, C.; Hancock, A. A. Medicinal chemistry and biological properties of non-imidazole histamine H_3 antagonists. *Mini-Rev. Med. Chem.* **2004**, *4*, 979–992. (c) Berlin, M.; Boyce, C. W. Recent advances in the development of histamine H_3 antagonists. *Exp. Opin. Ther. Pat.* **2007**, *17*, 675–687.

(13) Esbenshade, T. A.; Fox, G. B.; Krueger, K. M.; Baranowski, J. L.; Miller, T. R.; Kang, C. H.; Denny, L. I.; Witte, D. G.; Yao, B. B.; Pan, J. B.; Faghih, R.; Bennani, Y. L.; Williams, M.; Hancock, A. A. Pharmacological and behavioral properties of A-349821, a selective and potent human histamine H_3 receptor antagonist. *Biochem. Pharmacol.* **2004**, *68*, 933–945.

(14) Hancock, A. A.; Diehl, M. S.; Faghih, R.; Bush, E. N.; Krueger, K. M.; Krishna, G.; Miller, T. R.; Wilcox, D. M.; Nguyen, P.; Pratt, J. K.; Cowart, M. D.; Esbenshade, T. A.; Jacobson, P. B. In vitro optimization of structure activity relationships of analogues of A-331440 combining radioligand receptor binding assays and micronucleus assays of potential antiobesity histamine H_3 receptor antagonists. *Basic Clin. Pharmacol. Toxicol.* **2004**, *95*, 144–152.

(15) (a) Cowart, M.; Faghih, R.; Curtis, M. P.; Gfesser, G. A.; Bennani, Y. L.; Black, L. A.; Pan, L.; Marsh, K. C.; Sullivan, J. P.; Esbenshade, T. A.; Fox, G. B.; Hancock, A. A. 4-(2-[2-(2(*R*)-methylpyrrolidin-1-yl)ethyl]benzofuran-5-yl)benzonitrile and related 2-aminoethylbenzofuran H_3 receptor antagonists potently enhance cognition and attention. *J. Med. Chem.* **2005**, *48*, 38–55. (b) Esbenshade, T. A.; Fox, G. B.; Krueger, K. M.; Miller, T. R.; Kang, C. H.; Denny, L. I.; Witte, D. G.; Yao, B. B.; Pan, L.; Wetter, J.; Marsh, K.; Bennani, Y. L.; Cowart, M. D.; Sullivan, J. P.; Hancock, A. A. Pharmacological properties of ABT-239 [4-(2-{2-[(2*R*)-2-Methylpyrrolidinyl]ethyl}-benzofuran-5-yl)benzonitrile]: I. Potent and selective histamine H_3 receptor antagonist with drug-like properties. *J. Pharmacol. Exp. Ther.* **2005**, *313*, 165–175. (c) Fox, G. B.; Esbenshade, T. A.; Pan, J. B.; Radek, R. J.; Krueger, K. M.; Yao, B. B.; Browman, K. E.; Buckley, M. J.; Ballard, M. E.; Komater, V. A.; Miner, H.; Zhang, M.; Faghih, R.; Rueter, L. E.; Bitner, R. S.; Drescher, K. U.; Wetter, J.; Marsh, K.; Lemaire, M.; Porsolt, R. D.; Bennani, Y. L.; Sullivan, J. P.; Cowart, M. D.; Decker, M. W.; Hancock, A. A. Pharmacological properties of ABT-239 [4-(2-{2-[(2*R*)-2-methylpyrrolidinyl]ethyl}-benzofuran-5-yl)benzonitrile]: II. neurophysiological characterization and broad preclinical efficacy in cognition and schizophrenia of a potent and selective histamine H_3 receptor antagonist. *J. Pharmacol. Exp. Ther.* **2005**, *313*, 176–190.

(16) Hancock, A. A. The challenge of drug discovery of a GPCR target: analysis of preclinical pharmacology of histamine H_3 antagonists/inverse agonists. *Biochem. Pharmacol.* **2006**, *71*, 1103–1113.

(17) (a) Nagase, T.; Mizutani, T.; Ishikawa, S.; Sekino, E.; Sasaki, T.; Fujimura, T.; Ito, S.; Mitobe, Y.; Miyamoto, Y.; Yoshimoto, R.; Tanaka, T.; Ishihara, A.; Takenaga, N.; Tokita, S.; Fukami, T.; Sato, N. Synthesis, structure−activity relationships, and biological profiles of a quinazolinone class of histamine H_3 receptor inverse agonists. *J. Med. Chem.* **2008**, *51*, 4780–4789. (b) Thompson Reuters Integrity, MK-0249, Entry 433171, 2011.

(18) (a) Ligneau, X.; Landais, L.; Perrin, D.; Piriou, J.; Uguen, M.; Denis, E.; Robert, P.; Parmentier, R.; Anaclet, C.; Lin, J. S.; Burban, A.; Arrang, J. M.; Schwartz, J. C. Brain histamine and schizophrenia: potential therapeutic applications of H_3 receptor inverse agonists studied with BF2.649. *Biochem. Pharmacol.* **2007**, *73*, 1215–1224. (b) Ligneau, X.; Perrin, D.; Landais, L.; Camelin, J. C.; Calmels, T. P.; Berrebi-Bertrand, I.; Lecomte, J. M.; Parmentier, R.; Anaclet, C.; Lin, J. S.; Bertaina-Anglade, V.; la Rochelle, C. D.; d'Aniello, F.; Rouleau, A.; Gbahou, F.; Arrang, J. M.; Ganellin, C. R.; Stark, H.; Schunack, W.; Schwartz, J. C. BF2.649 [1-{3-[3-(4-chlorophenyl)-propoxy]propyl}piperidine, hydrochloride], a nonimidazole inverse agonist/antagonist at the human histamine H_3 receptor: preclinical pharmacology. *J. Pharmacol. Exp. Ther.* **2007**, *320*, 365–75.

(19) (a) Medhurst, A. D.; Atkins, A. R.; Beresford, I. J.; Brackenborough, K.; Briggs, M. A.; Calver, A. R.; Cilia, J.; Cluderay, J. E.; Crook, B.; Davis, J. B.; Davis, R. K.; Davis, R. P.; Dawson, L. A.; Foley, A. G.; Gartlon, J.; Gonzalez, M. I.; Heslop, T.; Hirst, W. D.; Jennings, C.; Jones, D. N.; Lacroix, L. P.; Martyn, A.; Ociepka, S.; Ray, A.; Regan, C. M.; Roberts, J. C.; Schogger, J.; Southam, E.; Stean, T. O.; Trail, B. K.; Upton, N.; Wadsworth, G.; Wald, J. A.; White, T.; Witherington, J.; Woolley, M. L.; Worby, A.; Wilson, D. M. GSK189254, a novel H_3 receptor antagonist that binds to histamine H3 receptors in Alzheimer's disease brain and improves cognitive performance in preclinical models. *J. Pharmacol. Exp. Ther.* **2007**, *321*, 1032–1045. (b) Thompson Reuters Integrity, GSK-189254, Entry 376370, 2011.

(20) (a) Wermuth, C. G.; Schlewer, G.; Bourguignon, J. J.; Maghioros, G.; Bouchet, M. J.; Moire, C.; Kan, J. P.; Worms, P.; Biziere, K. 3-Aminopyridazine derivatives with atypical antidepressant, serotonergic, and dopaminergic activities. *J. Med. Chem.* **1989**, *32*, 528–537. (b) Coates, W. J.; McKillop, A. One-pot preparation of 6-substituted 3(2*H*)-pyridazinones from ketones. *Synthesis* **1993**, 334–342.

(21) Curran, W. V.; Ross, A. 6-Phenyl-4,5-dihydro-3(2*H*)-pyridazinones. A series of hypotensive agents. *J. Med. Chem.* **1974**, *17*, 273–281.

(22) (a) Sircar, I.; Duell, B. L.; Bobowski, G.; Bristol, J. A.; Evans, D. B. Cardiotonic agents. 2. Synthesis and structure−activity relationships of 4,5-dihydro-6-[4-(1*H*-imidazol-1-yl)phenyl]-3(2*H*)-pyridazinones: a new class of positive inotropic agents. *J. Med. Chem.* **1985**, *28*, 1405–1413. (b) Sotelo, E.; Ravina, E. Efficient aromatization of 4,5-dihydro-3(2*H*)-pyridazinone substituted at 5 position by using anhydrous copper chloride. *Synth. Commun.* **2000**, *30*, 1–7.

(23) (a) Kodavanti, U. P.; Mehendale, H. M. Cationic amphiphilic drugs and phospholipid storage disorder. *Pharmacol. Rev.* **1990**, *42*, 327–354. (b) Ploemen, J. P.; Kelder, J.; Hafmans, T.; van de Sandt, H.; van Burgsteden, J. A.; Saleminki, P. J.; van Esch, E. Use of physicochemical calculation of pKa and CLogP to predict phospholipidosis-inducing potential: a case study with structurally related piperazines. *Exp. Toxicol. Pathol.* **2004**, *55*, 347–355.

(24) Bacon, E. R.; Bailey, T. R.; Becknell, N. C.; Chatterjee, S.; Dunn, D.; Hostetler, G. A.; Hudkins, R. L.; Josef, K. A.; Knutsen, L.; Tao, M.; Zulli, A. L. US2010273779, 2010.

(25) (a) Hopkins, A. L.; Groom, C. R.; Alex, A. Ligand efficiency: a useful metric for lead selection. *Drug Discovery Today* **2004**, *9*, 430–431. (b) Lesson, P. D.; Springthorpe, B. The influence of drug-like concept on decision-making in medicinal chemistry. *Nat. Rev. Drug Discovery* **2007**, *6*, 881–890. (c) Perola, E. An analysis of the binding efficiencies of drugs and their leads in successful drug discovery program. *J. Med. Chem.* **2010**, *53*, 2986–2997.

(26) (a) Menear, K. A.; Adcock, C.; Boulter, R.; Cockcroft, X. L.; Copsey, L.; Cranston, A.; Dillon, K. J.; Drzewiecki, J.; Garman, S.; Gomez, S.; Javaid, H.; Kerrigan, F.; Knights, C.; Lau, A.; Loh, V. M., Jr.; Matthews, I. T.; Moore, S.; O'Connor, M. J.; Smith, G. C.; Martin, N. M. 4-[3-(4-Cyclopropanecarbonylpiperazine-1-carbonyl)-4-fluorobenzyl]-2*H*-phthalazin-1-one: a novel bioavailable inhibitor of poly(ADP-ribose) polymerase-1. *J. Med. Chem.* **2008**, *51*, 6581–6591. (b) Hoelder, S.; Mueller, G.; Schoenafinger, K.; Will, D. W.; Matter, H.; Bossart, M. Preparation of Pyridazinones as Glycogen Synthase Kinase-3 Beta Inhibitors for Pharmaceutical Uses. WO2005111018, 2005.

(27) Yazdanian, M.; Glynn, S. L.; Wright, J. L.; Hawi, A. Correlating partitioning and caco-2 cell permeability of structurally diverse small molecular weight compounds. *Pharm. Res.* **1998**, *15*, 1490–1494.

(28) (a) Summerfield, S. G.; Stevens, A. J.; Cutler, L.; del Carmen Osuna, M.; Hammond, B.; Tang, S. P.; Hersey, A.; Spalding, D. J.; Jeffrey, P. Improving the in vitro prediction of in vivo central nervous system penetration: integrating permeability, P-glycoprotein efflux, and free fractions in blood and brain. *J. Pharmacol. Exp. Ther.* **2006**, *316*, 1282–1290. (b) Kalvass, J. C.; Olson, E. R.; Cassidy, M. P.; Selley, D. E.; Pollack, G. M. Pharmacokinetics and pharmacodynamics of seven opioids in P-glycoprotein-competent mice: assessment of unbound brain EC50, u and correlation of in vitro, preclinical, and clinical data. *J. Pharmacol. Exp. Ther.* **2007**, *323*, 346–355.

(29) Obach, R. S.; Baxter, J. G.; Liston, T. E.; Silber, B. M.; Jones, B. C.; MacIntyre, F.; Rance, D. J.; Wastall, P. The prediction of human pharmacokinetic parameters from preclinical and in vitro metabolism data. *J. Pharmacol. Exp. Ther.* **1997**, *283*, 46–58.

(30) Raucy, J.; Warfe, L.; Yueh, M. F.; Allen, S. W. A cell-based reporter gene assay for determining induction of CYP3A4 in a high-volume system. *J. Pharmacol. Exp. Ther.* **2002**, *303*, 412–423.

(31) Lagrutta, A. A.; Trepakova, E. S.; Salata, J. J. The hERG channel and risk of drug-acquired cardiac arrhythmia: an overview. *Curr. Top Med. Chem.* **2008**, *8*, 1102–1112.

(32) Clapham, J.; Kilpatrick, G. J. Histamine H_3 receptor-mediated modulation of water consumption in the rat. *Eur. J. Pharmacol.* **1993**, *232*, 99–103.

(33) Fox, G. B.; Pan, J. B.; Radek, R. J.; Lewis, A. M.; Bitner, R. S.; Esbenshade, T. A.; Faghih, R.; Bennani, Y. L.; Williams, M.; Yao, B. B.; Decker, M. W.; Hancock, A. A. Two novel and selective nonimidazole H_3 receptor antagonists A-304121 and A-317920: II. In vivo behavioral and neurophysiological characterization. *J. Pharmacol. Exp. Ther.* **2003**, *305*, 897–908.

(34) Raddatz, R.; Hudkins, R. L.; Mathiasen, J. R.; Gruner, J. A.; Le, S.; Schaffhauser, H.; Bozyczko-Coyne, D.; Marino, M. J.; Ator, M. A.; Bacon, E. R.; Mallamo, J. P.; Williams, M. Unpublished results.

(35) Irwin, S. Comprehensive observational assessment: Ia. A systematic quantitative procedure for assessing the behavioural and physiologic state of the mouse. *Psychopharmacologia* **1968**, *13*, 222–257.